Available online at www.sciencedirect.com

SciVerse ScienceDirect

Geochimica et Cosmochimica Acta 104 (2013) 165–182

Geochimica et Cosmochimica Acta

www.elsevier.com/locate/gca

Preservation and detection of microstructural and taxonomic correlations in the carbon isotopic compositions of individual Precambrian microfossils

Kenneth H. Williford [a,*], Takayuki Ushikubo [a], J. William Schopf [b,c], Kevin Lepot [a,1], Kouki Kitajima [a], John W. Valley [a]

[a] NASA Astrobiology Institute, WiscSIMS, Department of Geoscience, University of Wisconsin, 1215 W. Dayton St., Madison, WI 53706, USA
[b] Department of Earth and Space Sciences, Center for the Study of Evolution and the Origin of Life, and Molecular Biology Institute, University of California, Los Angeles, CA 90095, USA
[c] NASA Astrobiology Institute, Penn State Astrobiology Research Center, University Park, PA 16802, USA

Received 21 February 2012; accepted in revised form 2 November 2012; Available online 28 November 2012

Abstract

Here we present techniques for, and new data from, in situ carbon isotope ($\delta^{13}C$) analysis of Precambrian permineralized microscopic fossils with a reproducibility of 1–2‰ using secondary ion mass spectrometry (SIMS). Individual microfossils, selected for their excellent preservation, were analyzed in petrographic thin sections of stromatolitic cherts from the Proterozoic Gunflint (~1880 Ma), Bitter Springs (~830 Ma), Min'yar (~740 Ma), and Chichkan (~775 Ma) Formations. The range of $\delta^{13}C$ values (−34.6‰ to −22.1‰ VPDB) among the 46 individuals analyzed falls within that expected for photoautotrophic carbon fixation by ribulose bisphosphate carboxylase (RuBisCO), consistent with morphology-based taxonomic assignments for these specimens. Microfossils classified as cyanobacteria from the Gunflint, Bitter Springs, and Min'yar Formations (for which published carbonate carbon isotope data can be used to estimate the $\delta^{13}C$ of the original dissolved inorganic carbon substrate) exhibit a consistent ~19‰ total fractionation ($\delta^{13}C$ of dissolved inorganic carbon − $\delta^{13}C$ of biomass) similar to that observed in living cyanobacteria, over a wide range of $\delta^{13}C_{carb}$ values (−2.9‰ to 3.4‰). In stromatolitic chert of the Min'yar Formation, morphologically diverse microfossils preserved in a ~1 mm^2 part of a microbial mat exhibit systematic isotopic differences among and within taxa that correlate with their morphologically inferred biological affinities and suggest that isotopic signatures of their original biosynthetic processes (e.g., lipid and peptidoglycan synthesis) are preserved. Isotopic offsets consistent with the different RuBisCO-based fractionations typical of cyanobacteria and photosynthetic eukaryotes are documented by the differing $\delta^{13}C$ values of a colonial cyanobacterium (−22.6 ± 0.5‰) and a phytoplanktonic protistan acritarch (−28.9 ± 1.0‰) situated <1 cm apart in the stromatolitic Chichkan chert. These findings show for the first time the possibility of using in situ isotopic microanalysis of fossil microbial mats and ancient sediments in order to distinguish metabolic fingerprints within complex microbial ecosystems and consortia.
Published by Elsevier Ltd.

1. INTRODUCTION

The vast majority of Earth's genetic and metabolic diversity exists in the microbial realm (Pace, 1997), and microbes largely define the limits of environmental tolerance for life as we know it (Rothschild and Mancinelli, 2001). Although microbial life has flourished for at least three quarters of Earth history – most prominently, during the

* Corresponding author. Present address: Jet Propulsion Laboratory, California Institute of Technology, Pasadena, CA 91109, USA. Tel.: +1 912 344 5677; fax: +1 608 262 0693.
E-mail address: Kenneth.H.Williford@jpl.nasa.gov (K.H. Williford).
[1] Present address: Université Lille 1, Laboratoire Géosystèmes, CNRS UMR8217, 59655 Villeneuve d'Ascq, France.

0016-7037/$ - see front matter Published by Elsevier Ltd.
http://dx.doi.org/10.1016/j.gca.2012.11.005

Precambrian Eon of geological time – the familiar fossil record of large, morphologically diverse, and truly multicellular organisms of the Phanerozoic encompasses little more than one-tenth. Given Earth's fossil record and the extraordinary set of circumstances (including the vast expanse of time) required for large, multicellular life to have evolved on Earth, fossil evidence of extraterrestrial life (such as that sought in Mars rocks) is likely to be microbial (Ward and Brownlee, 2000).

The principle problem in evaluating any such putative fossils will be establishment of their biogenicity. As studies of Precambrian microfossils have shown (Schopf et al., 2010a), although morphology is a key element in such assessments, it reveals little conclusive information about modes of life such as metabolism. Although chemical analysis of individual microbial fossils or putative fossils can reveal such information, it presents significant technical challenges. Carbon isotope analysis of microbial fossils is particularly promising in this regard, given the preferential preservation of fossil carbon relative to other biologically important elements, and it can be used to assess biogenicity, metabolism, taxonomy, taphonomy, and paleoenvironmental conditions (House et al., 2000; Ueno et al., 2001; Kaufman and Xiao, 2003; Wacey et al., 2011).

Here we review previous efforts to measure the carbon isotopic compositions of individual microfossils, discuss the challenges and techniques involved, and present new carbon isotope data from four Proterozoic stromatolitic microbial assemblages exceptionally well preserved by permineralization in chert. We report our detection of microstructural (anatomic) and taxonomic correlations in the carbon isotopic composition of these individual Precambrian microfossils, and we demonstrate that the different photosynthetic fractionation effects associated with microorganisms of the bacterial and eukaryotic domains can be preserved on billion year time scales. Correlations between morphology and carbon isotopic composition such as those reported here, if observed in putative microfossils from early Earth or extraterrestrial samples, would be powerful indicators of biogenicity.

1.1. Previous work

The development of ion microprobes employing secondary ion mass spectrometry (SIMS) has enabled in situ measurement of isotope ratios at the micrometer scale, with sample sizes 10^4 to 10^9 times smaller in mass than conventional, "bulk" or "whole rock" techniques. The first reported carbon isotope measurements within individual cells, of the spatial distribution of ^{14}C-labeled arginine in cultured human fibroblasts, were made 20 years ago using the Cameca IMS 300 and IMS 3f (Hindie et al., 1992). In more recent years, spatial resolution, precision, and accuracy have improved, but the basic principles of the analytical technique have not changed since that time: in a high vacuum sample chamber, a "primary" ion (e.g., $^{133}Cs^+$) beam focused on the surface of a sample, results in the sputtering of sample-derived ions that are electrostatically focused into a "secondary" beam and then filtered by mass-to-charge ratio and measured (Kita et al., 2009).

Pioneering in situ carbon isotopic measurements were made on microfossils preserved in cherts of the Gunflint Formation of Ontario, Canada (~1880 Ma; (Fralick et al., 2002) and the Bitter Springs Formation of central Australia (~830 Ma (Walter et al., 2000) using the CAMECA IMS 1270 at the University of California, Los Angeles (House et al., 2000). If $\delta^{13}C$ of carbonates associated with microfossiliferous cherts is assumed to record the $\delta^{13}C$ of the available dissolved inorganic carbon (DIC) substrate, the $\delta^{13}C$ of microfossils ($\delta^{13}C_{org}$) can be used to evaluate their total metabolic fractionation ($\Delta^{13}C = \delta^{13}C_{DIC} - \delta^{13}C_{org}$). On the basis of morphology, the 15 Bitter Springs microfossils analyzed by House et al. (2000) had been previously classified as cyanobacteria (Schopf, 1968; Schopf and Blacic, 1971), an assignment supported by the carbon isotope data showing that the fractionations preserved were consistent with carbon fixation via the Calvin cycle ($\Delta^{13}C_{DIC-org} = 20–35‰$) or the acetyl-CoA pathway, but not the 3-hydroxyproprionate or reverse-TCA cycles ($\Delta^{13}C_{DIC-org} < 20‰$; House et al., 2000). All but two of the 15 microfossils analyzed from the Gunflint Formation also had carbon isotope ratios consistent with carbon fixation via the Calvin cycle (the two morphologically degraded outliers having appreciably lower $\delta^{13}C$). Notably, the carbon isotopic values of virtually all of the fossils analyzed from the two formations were within the range measured on bulk samples of kerogen from each of the units, providing strong support for the use of SIMS in such analyses (House et al., 2000).

Recent stratigraphic, petrographic and geochemical work on the Gunflint and other contemporaneous iron formations suggests that some of the microfossils in these units may preserve iron-metabolizing organisms rather than cyanobacteria (Planavsky et al., 2009; Wilson et al., 2010). There is also some evidence that carbon fixation by iron oxidizing bacteria could produce the low $\delta^{13}C$ values (House et al., 2000; this study) measured in Gunflint Fm microfossils (Kennedy et al., 2010). Kennedy et al. (2010) reported $\delta^{13}C$ of bacteriogenic ferrihydrite, but assumed a $\delta^{13}C$ of $-7‰$ for the dissolved CO_2 available to the organisms, and thus awaits confirmation by laboratory experiments including $\delta^{13}C$ measurements of metabolic substrates. Nonetheless, these results highlight the need for caution (and ideally, a detailed stratigraphic, petrographic, and geochemical context) when assigning taxonomic affinity to Precambrian microfossils based upon morphology and $\delta^{13}C$.

Standardization of measurements is critical for establishing the accuracy of SIMS analyses, a problem presented chiefly by systematic biases – sometimes called "instrumental mass fractionation" – that occur during analysis. Such "bias" can be measured and corrected by bracketing sample analyses with analyses of a working standard (or series of standards) of known isotopic composition and with a chemical composition similar to that of the sample (e.g., Eiler et al., 1997; Kita et al., 2009). In minerals, crystal structure and orientation can also affect bias (Huberty et al., 2010; Kozdon et al., 2010): for example, a ~3‰ orientation effect has been observed in graphite (Ushikubo, unpublished data). There is also evidence that the bias for

graphite, a crystalline material, is different than that for disordered organic matter. Consistent with earlier results by McKeegan et al. (1985), which reported a ~4‰ difference in bias for SIMS carbon isotope analysis of graphite and kerogen, House et al. (2000) identified a ~10‰ difference in bias between graphite and coal, and on that basis selected an Archean carbonaceous chert (containing a mixture of quartz and particulate kerogen) as a working standard for microfossil analyses. In contrast, it should be noted that the three SIMS carbon isotopic studies discussed below that have appeared since the House et al. (2000) work used crystalline standards (graphite or diamond) rather than structurally disordered particulate kerogen preserved in chert like that comprising permineralized organic-walled microfossils.

Ueno et al. (2001) analyzed putative microfossils and kerogen clots from a ~3.5 Ga chert-barite unit of the Warrawoona Group in the Pilbara Craton, Western Australia, concluding on the basis of $\delta^{13}C$ values ranging from −42‰ to −32‰ that the carbon in these structures was biogenic and fixed by the Calvin cycle or reductive acetyl-CoA pathway. Kaufman and Xiao (2003) used in situ carbon isotope analyses of individual ~1.4 Ga organic-walled microfossils of uncertain taxonomic, but presumably planktonic, affinity (acritarchs) to estimate that the atmospheric CO_2 concentration in the Mesoproterozoic was >10–200 times the present atmospheric level, based on the observation that Calvin cycle-using modern smaller-celled phytoplankton in laboratory cultures exhibit a maximum fractionation ($\Delta^{13}C_{DIC-org}$) of ≈ 25‰ at atmospheric CO_2 concentrations 8–10 times the present level that could have been enhanced in the fossils by their significantly larger apparent volume to surface ratio. Most recently, Wacey et al. (2011) reported carbonaceous tubular and spheroidal microfossils, inferred to be fossil sulfur-processing bacteria, from the basal sandstone of the ~3.4 Ga Strelley Pool Formation of Western Australia. In situ carbon isotope measurements of these microfossils by SIMS (standardized with graphite) range in $\delta^{13}C$ from −46‰ to −33‰ (Wacey et al., 2011).

2. SAMPLES AND METHODS

2.1. Description of samples and standards

2.1.1. Samples

Seven petrographic thin sections (~75–200 μm thickness) of stromatolitic fossiliferous cherts from the Gunflint, Bitter Springs, Min'yar, and Chichkan Formations were selected for this study. Within these, 14 areas containing one or more microbial fossils located at or near the surface of the section were identified, assigned a sample code (e.g., in a Gunflint Formation section, sample code GUN-1 containing specimens of *Gunflintia* and *Huroniospora*; these codes are used throughout) and photomicrographed in transmitted light. Basic geologic, geochronologic, and geochemical information about the four microfossiliferous units is given in Table 1. Table 2 lists sample codes and corresponding thin sections; photomicrographs of all microfossils analyzed and all analytical pits, in addition to those shown in the text-figures, are provided in Supplementary information (SI).

2.1.2. Standards

To continue the search for an appropriate working standard for the SIMS analysis of carbon isotopes in permineralized microfossils, carbonaceous cherts from four Precambrian geologic units were evaluated by SIMS at a

Table 1
Information about fossiliferous units studied (after Schopf et al., 2005, except where noted). RIP refers to the Raman Index of Preservation (Schopf et al., 2005).

Geologic unit; locality	Estimated age (Ma)	Metamorphic grade	RIP	H/C	TOC (mg/g)	$\delta^{13}C_{org}$ (‰, VPDB)	$\delta^{13}C_{carb}$ (‰, VPDB)
Chichkan Formation; Ayusakan, Kazakhstan	775 (800–750)[d]	Laumonite–prehnite–pumpellyite	8.6	*n.d.*	0.16 to 0.76[a]	−28.4 $n = 2$ (−28.9 to −27.9)[a]	*n.d.*
Min'yar Formation; Bashkiria, Russia	740	Laumonite–prehnite–pumpellyite	8.8	*n.d.*	0.78[a]	−29.4[a]	1.3[c]
Bitter Springs Formation; Northern Territory, Australia	830	*n.d.*	9.0	0.43 $n = 8$ (0.10 to 0.82)	0.19 $n = 38$ (0.16 to 0.65)[a]	−25.8 $n = 43$ (−28.8 to −15.8)[a]	3.4[b]
Gunflint Formation; Ontario, Canada	1880	Subgreenschist	8.8	0.40 $n = 7$ (0.10 to 0.61)	0.46 $n = 72$ (0.4 to 16.06)[a]	−32.6 $n = 57$ (−35.6 to −18.3)[a]	−2.9[b]

[a] Strauss et al. (1992).
[b] Strauss and Moore (1992).
[c] Podkovyrov et al. (1998).
[d] Sergeev and Schopf (2010)

Table 2
Sample information. Sample column lists codes for microfossiliferous regions dissected from thin sections and then epoxy mounted for SIMS analysis. Comments column lists informal names used to identify microfossiliferous areas.

Formation	Sample	Slide	Comments
Gunflint	GUN-1	GF-Sch-4B	*Gunflintia* and *Huroniospora*
Gunflint	GUN-2	GF-Sch-8A	*Gunflintia*
Gunflint	GUN-3	GF-Sch-8A	*Gunflintia* and *Huroniospora*
Gunflint	GUN-4	GF-Sch-8A	*Gunflintia*
Gunflint	GUN-5	GF-Sch-8A	*Huroniospora*
Bitter Springs	BIT-SPR-1	Bit Spr 1327-1A	Spot cell colony
Bitter Springs	BIT-SPR-2	Bit Spr 1327-1C	Cells in layer
Bitter Springs	BIT-SPR-3	Bit Spr 1327-1C	Good cells at surface
Min'yar	MIN-3	Min'yar $R_{3mn(ST)}$-2J	Excellent sphere colony
Chichkan	CHICH-1	Chichkan 4681-68B 7A-2	Sheath
Chichkan	CHICH-2	Chichkan 4681-68B 7A-2	Excellent cell filament
Chichkan	CHICH-3	Chichkan 4681-68B 7A-2	Single cell
Chichkan	CHICH-5	Chichkan 4681-68B 7A-1	Brown cell
Chichkan	CHICH-6	Chichkan 4681-68B 7A-1	Cell cluster

micrometer-scale to determine the spatial heterogeneity in carbonaceous content and $\delta^{13}C$; none was found to have the appropriate combination of kerogen content and isotopic homogeneity required of a working standard. Evaluation of other Precambrian carbonaceous cherts continues at WiscSIMS, in order to identify a suite of isotopically homogeneous, low total organic carbon (TOC) working standards that exhibit an appropriate range of H/C. For this study, however, we used an epoxy-embedded chip of carbonaceous chert sample PPRG-215-1 (Walter et al., 1983) provided by House, the same working standard used by House et al. (2000) to measure carbon isotope compositions of Gunflint and Bitter Springs Formation microfossils, and the use of which thus allows an interlaboratory comparison of our results with those previously reported.

2.2. Sample preparation

Subsequent to locating specimens for analysis and their photomicrography, described above, ~1 mm^2 areas containing microfossils were dissected from thin sections by use of a low speed, water-cooled diamond saw (Buehler IsoMet). These fragments were cleaned by rinsing in acetone and isopropyl alcohol and arranged face down on double-sided transparent tape within a 1-cm-diameter area. The fragments were oriented to be as nearly coplanar as possible so that fossils exposed at their surfaces would not be differentially removed during final polishing of the sample mount. Each sample was then epoxy-embedded into a 2.54-cm-diameter plastic mold. After curing, each epoxy mount was removed from the mold and the surface to be analyzed was polished using a water-based suspension. The mounts were trimmed to a thickness of 5 mm, cleaned with dilute alkaline detergent, and sonicated sequentially: three times, each for 1 min, in deionized water, for 30 s in ethanol, and again twice, each for 30 s, in deionized water.

The microfossils to be analyzed in these mounts were then photomicrographed both in transmitted and reflected light. A thin (~5 nm) gold coat was applied to the mounts, and scanning electron microscope (SEM) images of the microfossils were acquired in backscattered electron (BSE) mode to document the distribution of organic carbon exposed at the surface in the areas to be analyzed. Finally, a thicker (~30 nm) gold coat was applied to facilitate charge distribution during SIMS analysis, and all samples were degassed for 48 h at 10^{-9} torr in the SIMS air-lock sample chamber prior to analysis.

2.3. Carbon isotope analysis

Carbon isotope analyses were performed on the WiscSIMS CAMECA IMS 1280 in the Department of Geoscience, University of Wisconsin, Madison. A $^{133}Cs^+$ primary ion beam having 20 kV total accelerating voltage and ~2.5 nA intensity was focused into an ellipse of ~15 μm maximum dimension at the sample surface. Secondary ion accelerating voltage was 10 kV. Simultaneous collection of $^{12}C^-$, $^{13}C^-$, and $^{13}CH^-$ ions was achieved using mass resolution of ~4000 on an axial electron multiplier (EM) for $^{13}C^-$, ~2200 on a Faraday cup (FC) at the L′2 position with a 10^{11} Ω resistor for $^{12}C^-$, and ~2200 on an EM at the H2 position for $^{13}CH^-$.

Multiple microfossils were analyzed in each sample mount during each SIMS session. Each time a sample was moved to a new microfossiliferous location, *X* and *Y* parameters of the deflector (DTFA) were adjusted to set the $^{12}C^-$ ion image in the center of the field aperture on an area near (within ~500 μm) the microfossils to be analyzed. To obtain a stable secondary ion image, a ~2.5 nA primary beam (with the same ~15 μm diameter as the analytical beam) was rastered over a 25 × 25 μm area, and voltage was applied to the dynamic transfer plates to deflect the secondary ions synchronized with primary beam rastering. After the adjustment of the DTFA-*X* and -*Y* values, the rastering beam was stopped, and carbon isotope analysis of microfossils began. Microfossil analyses consisted of 70 s of presputtering and a total counting time of 160 s (80 measurement cycles of 2 s each). Internal precision was calculated as two standard errors (SE) of $^{13}C/^{12}C$ ratios from the 80 cycles. Each set of ~10 sample analyses was bracketed with eight different spot analyses of the PPRG-215-1 standard, and external precision for each bracket

was calculated as two standard deviations (SD) of these eight standard analyses. Bias (α_{SIMS}) was calculated by comparing the average "raw" value ($\delta^{13}C_{Raw}$= $[(^{12}C/^{13}C)_{measured}/0.0112372 - 1] \times 1000$) for 8 bracketing analyses of PPRG-215-1 to the published value (−31.5‰ VPDB; Hayes et al., 1983) using the following equation:

$$\alpha_{SIMS} = (\delta^{13}C_{Raw} + 1000)/(-31.5 + 1000). \quad (1)$$

This factor, α, was used to correct raw values from sample analyses using the following equation (see also Kita et al., 2009):

$$\delta^{13}C_{PDB}(\text{sample}) = [(1 + \delta^{13}C_{RAW}(\text{sample})/1000/\alpha_{SIMS} - 1] \times 1000. \quad (2)$$

To illustrate the efficacy of this procedure, Fig. S1 (Supplementary information) shows a representative bracket compared with a bracket from a session analyzing $\delta^{13}C$ of amorphous Archean kerogen with a higher concentration of C, permitting use of a smaller, lower intensity beam and two FC detectors; this two FC detector technique enables the use of an anthracite coal as the working standard and results in higher precision (0.2‰, 2 SD) than the technique for microfossils.

3. RESULTS

3.1. Standards and analytical precision

During the analytical session from 7/29 to 7/31/2011, 75 sample analyses were made distributed over 8 brackets (i.e., four analyses of the standard before and after each set of ~10 sample analyses). Of these 75 analyses, 14 were "background" measurements made to assess ^{12}C count rate and $\delta^{13}C$ of any diffuse organic matter in non-fossiliferous chert near, but not including the microfossils to be analyzed, and to facilitate stabilization of the detector system after sample changes. In most cases, the first one or two analyses made after moving to a new microfossiliferous area were background analyses. The average ^{12}C count rate was 0.5×10^6 counts per second (cps) for these background analyses (compared to 3.3×10^6 cps for accepted sample analyses), indicating that diffuse organic matter generally contributes only a small amount of carbon to analyses of individual microfossils. Furthermore, for the background analyses that sampled enough carbon to obtain a meaningful isotope ratio (e.g., in the Gunflint Formation), the $\delta^{13}C$ of this material was very similar (±2‰) to the average $\delta^{13}C$ of associated microfossils, indicating that a small contribution of background organic matter would not significantly alter individual microfossil analyses. However, if background carbon has a significantly different $\delta^{13}C$ (e.g., 10‰) from individual microfossil carbon, then even a 15% contribution can bias a measurement to a degree equivalent to stated external precision (e.g., 1.5‰). Such an effect is apparent in analyses of fossils within the Chichkan Fm (see Section 4) that sampled a "background" phase morphologically and isotopically distinct from cell wall kerogen. In this case, the background phase was clearly identified in high-resolution SEM images of analytical pits.

To assess whether surface contamination introduced during sample preparation and handling (e.g., from epoxy or environmental hydrocarbons) was a factor, quartz within a microfossiliferous chert sample, but completely free from diffuse organic matter, was analyzed twice. Both of these analyses show a small peak in ^{12}C count rate of 700 cps (four orders of magnitude less than sample analyses) at 2 s, and fall rapidly below 20 cps within 30 s. Surface contamination is thus negligible, and any small amount that exists is completely removed during the presputtering phase of the analysis.

The average ^{12}C count rate for the 44 accepted analyses of the standard was 3.10×10^6 counts/s (for a total of 4.96×10^8 counts/analysis). Typically the first two analyses of the standard made after a sample change were rejected to allow the detector system to stabilize; all standard analyses with ^{12}C count rates less than 1×10^6 cps were also rejected. It should be noted that internal precision decreases significantly relative to external precision (the reproducibility of bracketing standards) at ^{12}C count rates below ~30% of the average for bracketing standards for these analytical conditions, largely due to Poisson counting statistics (Fig. S2, Supplementary information). For this reason, ^{12}C count rate relative to the average ^{12}C count rate of the corresponding bracketing standards ($^{12}C_{rel}$) is shown for each individual sample analysis as a percentage in Tables 3 and S1 (Supplementary information). Average ^{12}C count rate for the 57 accepted analyses of samples was 3.27×10^6 cps. We find no correlation between $^{12}C_{rel}$ and $\delta^{13}C$ (Fig. S11). A slight, apparent correlation in the Chichkan Fm (e.g., Fig. 7) is driven by analyses of at least three distinct categories of OM, clearly distinguishable in pre- and post-analysis images: amorphous, "background" OM (with low relative $\delta^{13}C$), acritarch biomass (low relative $\delta^{13}C$ and thick cell walls yielding high $^{12}C_{rel}$), and cyanobacterial biomass (high relative $\delta^{13}C$ and thin cell walls yielding low $^{12}C_{rel}$).

As noted above, external precision ("reproducibility") for each bracket was determined by calculating two standard deviations (2 SD) of the raw $\delta^{13}C$ value for the eight bracketing standard analyses; for the total of 44 accepted analyses of the standard, this value ranged from 1.3‰ to 2.7‰, with an average of 1.9‰. Internal precision was determined by calculating two standard errors (2 SE) of the raw $\delta^{13}C$ values acquired over 80 measurement cycles during each individual analysis. Internal precision can be affected by numerous factors, most notably the heterogeneous distribution or isotopic composition of organic carbon with depth in the material removed by sputtering during individual analyses. Average internal precision (2 SE) was 1.3‰ for the 44 accepted analyses of the standard and 1.6‰ for the 57 accepted measurements of the 46 microfossils analyzed.

For SIMS analysis of amorphous OM (e.g., kerogen and pyrobitumen) using a smaller (1–10 μm), less intense (0.015–0.5 nA) beam, a negative correlation has been observed between H/C of OM and instrumental bias (Sangély et al., 2005; Williford et al., 2011). When using those analytical conditions, we correct for this effect (over a total range of ~4‰ between low H/C shungite and high H/C ambers)

Table 3
Data from microfossil analyses listed by formation (See Table S1 for a summary of all measurements carried out, listed in the order of their acquisition). For sample codes, refer to Table 2. External precision (2 SD) is calculated as two standard deviations of the eight bracketing standard analyses corresponding to each sample analysis. Bias (α_{SIMS}) is calculated by comparing the average of $\delta^{13}C_{Raw}$ values for eight bracketing standard analyses to the expected value for the standard.

Date	Analysis	Sample	Taxon	$\delta^{13}C_{VPDB}$ (‰ VPDB)	±2 SD* (‰)	α_{SIMS}	Bias (‰)	$\delta^{13}C_{RAW}$ (‰)	±2 SE** (‰)	$^{13}CH/^{13}C$***	$^{12}C_{rel}$† (%)
Gunflint Formation											
08/01/15	@308	GUN-1	*Huroniospora microreticulata*	−32.0	2.7	0.964	−36.45	−67.31	0.95	0.101	95
08/01/15	@309	GUN-1	cf. *Huronispora* sp.	−29.8	2.7	0.964	−36.45	−65.12	1.00	0.092	139
08/01/15	@310	GUN-1	*Huronispora microreticulata*	−30.4	2.7	0.964	−36.45	−65.71	0.93	0.092	119
08/01/15	@311	GUN-1	*Gunflintia minuta*	−31.5	2.7	0.964	−36.45	−66.83	1.24	0.104	103
08/01/15	@312	GUN-1	clumped (cellular?) organic matter	−30.8	2.7	0.964	−36.45	−66.10	0.51	0.099	355
07/30/15	@59	GUN-2	*Gunflintia minuta*	−31.3	2.3	0.965	−34.74	−64.92	0.96	0.095	192
07/30/15	@61	GUN-2	*Huronispora microreticulata*	−30.5	2.3	0.965	−34.74	−64.19	1.07	0.118	248
07/30/15	@57	GUN-3	*Huronispora*	−32.5	2.3	0.965	−34.74	−66.13	0.79	0.089	235
07/30/15	@58	GUN-3	*Gunflintia minuta*	−32.4	2.3	0.965	−34.74	−66.01	1.38	0.112	106
08/01/15	@313	GUN-4	*Gunflintia minuta*	−30.9	2.7	0.964	−36.45	−66.24	1.51	0.097	46
07/30/15	@62	GUN-5	*Huronispora microreticulata*	−33.9	2.3	0.965	−34.74	−67.45	0.70	0.092	283
AVG				−31.4	2.5	0.964	−35.68	−66.00	1.00	0.099	175
Bitter Springs Formation											
07/30/15	@70	BIT-SPR-1	*Glenobotrydion aenigmatis*	−27.2	2.2	0.965	−34.78	−61.05	0.88	0.077	282
07/30/15	@72	BIT-SPR-1	*Eozygion minutum*	−24.3	2.2	0.965	−34.78	−58.25	1.00	0.071	186
07/30/15	@73	BIT-SPR-1	*Eozygion minutum*	−26.0	2.2	0.965	−34.78	−59.87	1.33	0.072	373
07/30/15	@74	BIT-SPR-2	cf. *Bigeminococcus mucidus*	−23.8	2.2	0.965	−34.78	−57.77	0.81	0.065	290
07/30/15	@75	BIT-SPR-2	cf. *Bigeminococcus mucidus*	−24.9	2.2	0.965	−34.78	−58.85	1.29	0.073	160
07/30/15	@76	BIT-SPR-2	cf. *Bigeminococcus mucidus*	−22.3	2.2	0.965	−34.78	−56.29	1.13	0.067	129
07/30/15	@77	BIT-SPR-3	cf. *Eozygion minutum*	−27.6	2.2	0.965	−34.78	−61.42	0.94	0.071	186
07/30/15	@78	BIT-SPR-3	cf. *Eozygion minutum*	−23.9	2.2	0.965	−34.78	−57.89	0.66	0.071	271
07/30/15	@79	BIT-SPR-3	cf. *Eozygion minutum*	−24.6	2.2	0.965	−34.78	−58.48	1.22	0.072	118
AVG				−25.0	2.2	0.965	−34.78	−58.87	1.03	0.071	222
Min'yar Formation											
07/31/15	@203	MIN-3	cf. *Gloeodiniopsis lamellosa*	−28.7	1.6	0.964	−35.85	−63.48	1.38	0.083	167
07/31/15	@204	MIN-3	*Eomycetopsis robusta*	−27.0	1.6	0.964	−35.85	−61.86	2.35	0.087	35
07/31/15	@205	MIN-3	cf. *Gloeodiniopsis lamellosa*	−30.9	1.6	0.964	−35.85	−65.63	2.22	0.090	37
07/31/15	@206	MIN-3	*Glenobotrydion majorinum*††	−34.6	1.6	0.964	−35.85	−69.22	2.49	0.090	57
07/31/15	@207	MIN-3	*Glenobotrydion majorinum*	−28.0	1.6	0.964	−35.85	−62.86	1.89	0.051	47
07/31/15	@208	MIN-3	cf. *Gloeodiniopsis lamellosa*	−28.5	1.6	0.964	−35.85	−63.33	1.37	0.070	98
07/31/15	@209	MIN-3	*Eomycetopsis robusta*	−25.5	1.6	0.964	−35.85	−60.39	1.17	0.062	124
07/31/15	@210	MIN-3	*Eomycetopsis robusta*	−25.3	1.6	0.964	−35.85	−60.28	1.43	0.061	101
07/31/15	@218	MIN-3	*Glenobotrydion majorinum*††	−28.6	1.3	0.964	−36.01	−63.55	1.74	0.060	50
07/31/15	@219	MIN-3	*Glenobotrydion majorinum*	−23.5	1.3	0.964	−36.01	−58.66	1.28	0.057	59
07/31/15	@220	MIN-3	*Glenobotrydion majorinum*	−24.8	1.3	0.964	−36.01	−59.92	1.84	0.046	39
07/31/15	@221	MIN-3	*Glenobotrydion majorinum*	−25.4	1.3	0.964	−36.01	−60.54	1.97	0.044	31
07/31/15	@222	MIN-3	*Glenobotrydion majorinum*	−26.9	1.3	0.964	−36.01	−61.98	1.79	0.052	40
07/31/15	@223	MIN-3	*Glenobotrydion majorinum*††	−28.2	1.3	0.964	−36.01	−63.22	1.95	0.072	66

07/31/15	@224	MIN-3	*Eomycetopsis robusta*	−25.0	1.3	0.964	−36.01	−60.13	1.87	0.075	31
07/31/15	@225	MIN-3	*Eomycetopsis robusta*	−24.5	1.3	0.964	−36.01	−59.67	1.95	0.066	31
08/01/15	@324	MIN-3	cf. *Gloeodiniopsis lamellosa* (low cps)	−28.3	2.8	0.964	−35.76	−63.06	2.19	0.083	20
08/01/15	@325	MIN-3	Mat surface	−23.8	2.8	0.964	−35.76	−58.74	1.29	0.070	82
08/01/15	@326	MIN-3	Mat surface	−26.8	2.8	0.964	−35.76	−61.56	0.81	0.060	149
08/01/15	@327	MIN-3	*Glenobotrydion aenigmatis*	−25.7	2.8	0.964	−35.76	−60.59	1.31	0.073	59
08/01/15	@328	MIN-3	*G. majorinum and Eozygion minutum*	−26.7	2.8	0.964	−35.76	−61.48	1.37	0.094	55
08/01/15	@329	MIN-3	*E. robusta and G. majorinum* (spot)	−28.5	2.8	0.964	−35.76	−63.25	2.07	0.080	31
AVG				−27.1	1.8	0.964	−35.88	−61.97	1.71	0.069	64
Chichkan Formation											
07/31/15	@168	CHICH-1	*Siphonopycus solidum*	−31.8	1.5	0.963	−36.92	−67.58	1.10	0.085	93
07/31/15	@169	CHICH-1	*Siphonopycus solidum*	−30.9	1.5	0.963	−36.92	−66.63	1.35	0.105	147
07/31/15	@182	CHICH-2	*Oscillatoriopsis media* (low cps)	−24.3	1.6	0.963	−37.05	−60.43	2.57	0.095	26
07/31/15	@183	CHICH-2	*Oscillatoriopsis media*	−29.2	1.6	0.963	−37.05	−65.15	1.76	0.083	58
07/31/15	@184	CHICH-2	*Oscillatoriopsis media* (low cps)	−26.0	1.6	0.963	−37.05	−62.13	2.46	0.104	23
07/31/15	@186	CHICH-2	*Oscillatoriopsis media* (low cps)	−25.9	1.6	0.963	−37.05	−61.95	2.67	0.099	24
07/31/15	@174	CHICH-3	*Leiosphaerida crassa*	−31.8	1.5	0.963	−36.92	−67.59	1.16	0.081	105
07/31/15	@175	CHICH-3	*Leiosphaerida crassa*	−29.8	1.5	0.963	−36.92	−65.58	1.30	0.083	80
07/31/15	@188	CHICH-5	*Leiosphaerida crassa*	−28.8	1.6	0.963	−37.05	−64.79	0.97	0.083	170
07/31/15	@189	CHICH-5	*Leiosphaerida crassa*	−29.9	1.6	0.963	−37.05	−65.81	2.78	0.097	28
07/31/15	@190	CHICH-5	*Leiosphaerida crassa*	−28.0	1.6	0.963	−37.05	−63.97	1.12	0.083	120
07/31/15	@192	CHICH-6	*Myxococcoides* sp.	−23.1	1.6	0.963	−37.05	−59.27	1.73	0.092	57
07/31/15	@193	CHICH-6	*Myxococcoides* sp.	−22.7	1.6	0.963	−37.05	−58.86	2.12	0.099	44
07/31/15	@194	CHICH-6	*Myxococcoides* sp.	−22.1	1.6	0.963	−37.05	−58.29	1.61	0.085	46
AVG				−27.4	1.6	0.963	−37.01	−63.43	1.76	0.091	73

[*] External precision (2 SD) is calculated as two standard deviations of $\delta^{13}C$ values from eight analyses of PPRG 215-1 standard bracketing each ~10 sample analyses.

[**] Internal precision (2 SE) is calculated as two standard errors of $\delta^{13}C$ values from 80 measurement cycles in each sample analysis.

[***] Mass 14 (^{13}CH) was measured simultaneously with ^{12}C and ^{13}C and used to calculate $^{13}CH/^{13}C$. See text for a discussion of a possible correlation between $^{13}CH/^{13}C$ and bias in SIMS analysis of preserved carbonaceous matter.

[†] Relative ^{12}C count rate ($^{12}C_{rel}$) for each sample analysis is listed as a percentage of the average ^{12}C count rate for eight bracketing standard analyses.

[††] With internal body.

using a suite of standard organic materials with known $\delta^{13}C$ and a wide range of H/C (Williford et al., 2011). Generally, only small corrections are required due to the close correspondence between the H/C of the working standard and samples. In order to test whether such an effect existed using the different analytical technique applied to $\delta^{13}C$ analysis of microfossils, we measured a suite of carbonaceous chert samples with known $\delta^{13}C$ and a wide range of H/C (the standard suite used for kerogen analysis mentioned above comprises materials whose carbon concentration would result in saturation of the electron multiplier when analyzed with a 2.5 nA beam intensity). No correlation between H/C and bias was observed in this experiment (Fig. S12), although it is possible that the spatial heterogeneity in $\delta^{13}C$ and H/C of the carbonaceous cherts used masks any such relation that does exist. Average $^{13}CH^-/^{13}C^-$ of microfossils in all four units studied here is slightly higher than that of the PPRG 215-1 standard (Supplementary data). If the correction procedure used for small spot kerogen analyses was applied in this study, the maximum correction would be ~1‰ for the range of $^{13}CH^-/^{13}C^-$ reported here. We report our measurements of $^{13}CH^-/^{13}C^-$ made simultaneously with each $\delta^{13}C$ analysis in the event that such an effect is observed in future experiments.

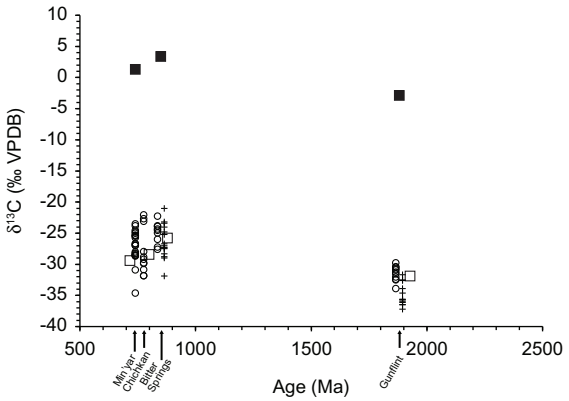

Fig. 1. Compilation of $\delta^{13}C$ values from marine carbonates (filled squares), bulk kerogen (open squares), and the in situ microfossil analyses reported here (open circles) and from an earlier study (crosses) by House et al. (2000). Carbonate data for Gunflint and Bitter Springs Formations from Strauss and Moore (1992), and for Min'yar Formation (Upper Subformation) from Podkovyrov et al. (1998). Average bulk kerogen data from Strauss et al. (1992).

3.2. Sample analyses

Table 3 presents a detailed summary of the carbon isotope data acquired from the 57 total analyses of 46 microfossils in four Proterozoic stromatolitic cherts reported here. Data from all analyses conducted in this study, ordered by their time of acquisition, are presented in Table S1 (SI).

3.2.1. Gunflint Formation

In the Gunflint Formation, the 11 microfossils exhibited $\delta^{13}C$ values ranging from −29.8‰ to −33.9‰. As is shown in Fig. 1, the average $\delta^{13}C$ of these specimens (−31.4‰) is similar to the average $\delta^{13}C$ of 57 analyses of bulk kerogen from the Gunflint Formation (−32.6‰; Strauss and Moore, 1992). As listed in Table 3, one clump of Gunflint organic matter and multiple specimens of two taxa of fossils were analyzed: four specimens of the benthic, narrow,

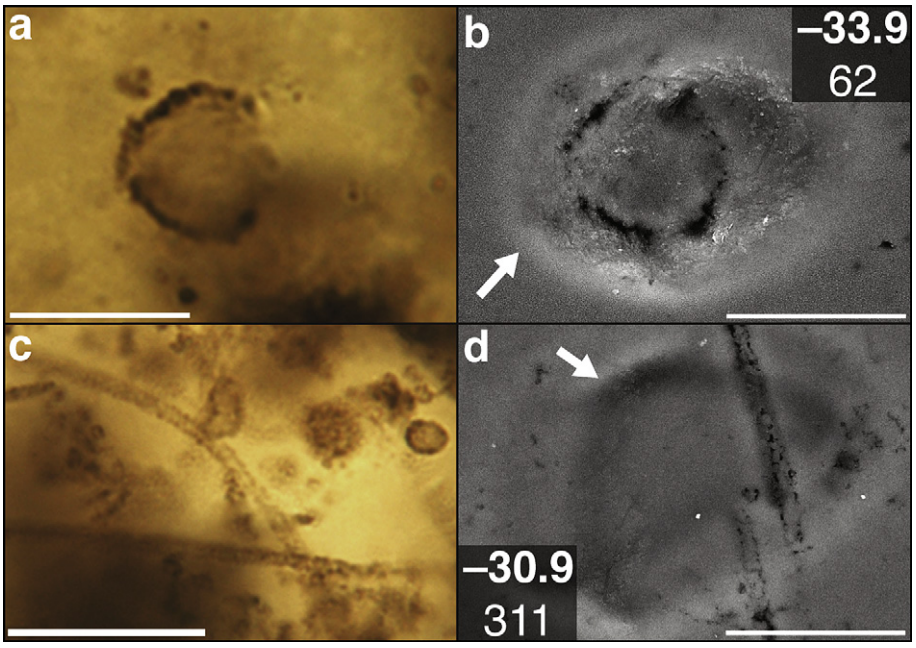

Fig. 2. Representative carbon isotope analyses of microfossils from the Gunflint Formation. Transmitted light micrographs (a, c) and backscattered electron micrographs (b, d) *Huroniospora* sp. (a, b), and *Gunflintia* sp. (c, d). Arrows indicate edges of SIMS analytical pits. Carbon isotope values (‰, VPDB) and individual analysis numbers are indicated in gray boxes, and scale bars represent 10 μm. (For the color version of this and following figures, the reader is referred to the web version of this article.)

filamentous cyanobacterium-like microbe *Gunflintia* (Fig. 2b), having an average $\delta^{13}C$ of −31.5‰ (ranging from −32.4‰ to −30.9‰), and six small-diameter planktonic cyanobacterium-like unicells assigned to *Huroniospora* (Fig. 2a) that have an average $\delta^{13}C$ of −31.7‰ (ranging from −33.9‰ to −29.8‰). The 10 Gunflint specimens measured in this study are isotopically similar to, but less variable and generally have higher $\delta^{13}C$ than the 16 Gunflint fossils measured by House et al. (2000), which had an average $\delta^{13}C$ value of −36.2‰ and ranged from −31.7‰ to −45.8‰ (Fig. 1).

3.2.2. Bitter Springs Formation

The nine microfossils analyzed from the Bitter Springs Formation, specimens of the coccoidal, commonly sheath-enclosed cyanobacterial taxa *Glenobotrydion*, cf. *Eozygion*, and cf. *Bigeminococcus* (Fig. 3), have $\delta^{13}C$ values ranging from −22.3‰ to −27.6‰. All analyses were made in a single bracket with an external precision of ±2.2‰ (2 SD). As shown in Fig. 1, the average $\delta^{13}C$ value of the nine specimens measured, −25.0‰, is closely comparable to the average $\delta^{13}C$ from 29 analyses of bulk kerogen from the formation (−25.8‰) (Strauss and Moore, 1992) (Fig. 1).

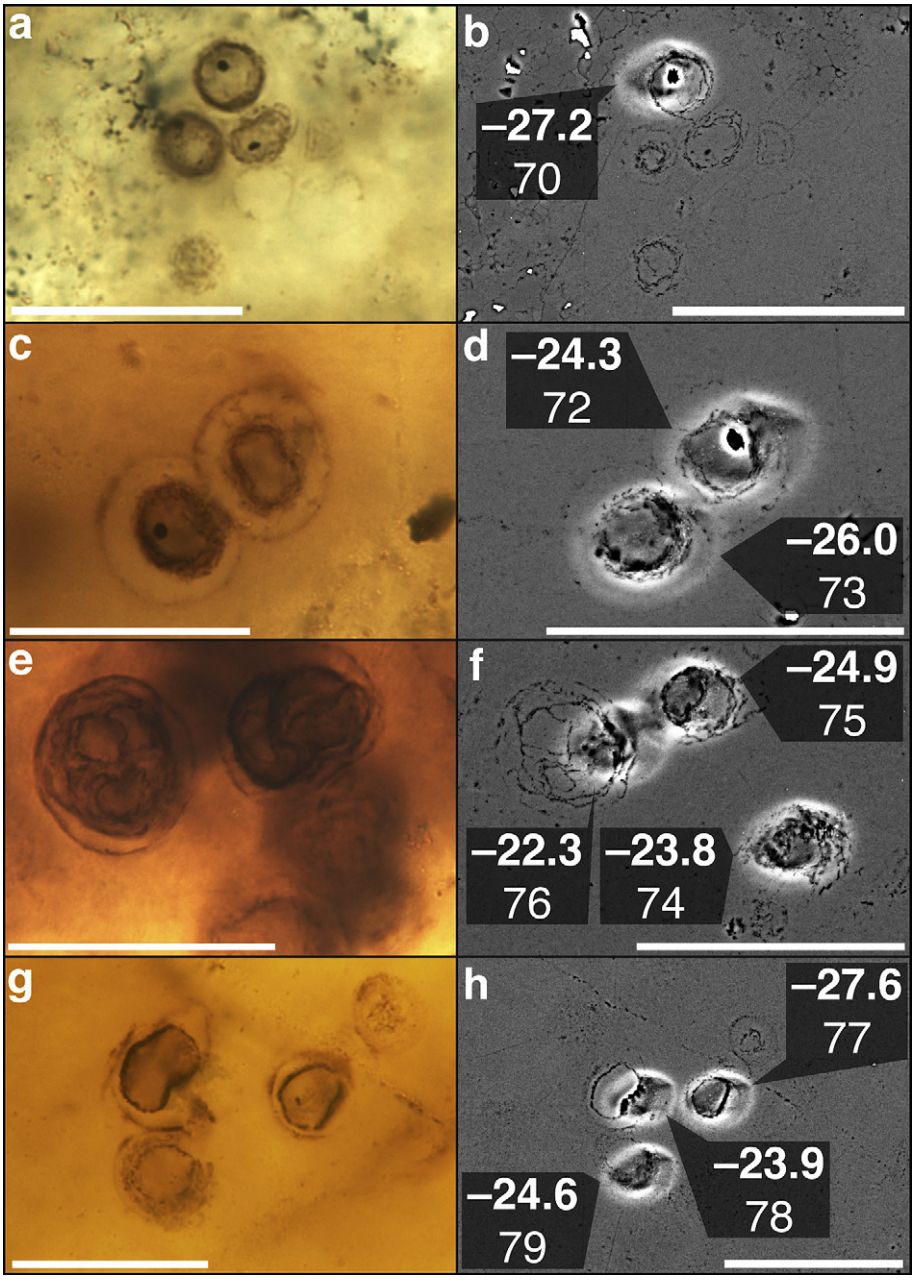

Fig. 3. Carbon isotope analyses of microfossils from the Bitter Springs Formation. Transmitted light images are shown in (a), (c), (e), and (g), and backscattered electron images (with SIMS analytical pits) are shown in (b), (d), (f), and (h). Carbon isotope ratios (‰, VPDB) and individual analysis numbers are shown in gray boxes; scale bars represent 20 μm.

Although only a single specimen of *Glenobotrydion aenigmatis* was measured ($\delta^{13}C = -27.2‰$; Fig. 3a and b), analyses of multiple specimens of the other Bitter Springs taxa provide a basis by which to assess intraspecific isotopic variability. Thus, for example, two immediately adjacent individuals of *Eozygion minutum* have $\delta^{13}C$ values of $-24.3‰$ and $-26.0‰$ (Fig. 3c and d); three specimens of cf. *Eozygion minutum*, less than 20 μm apart, have $\delta^{13}C$ values from $-23.9‰$ to $-27.6‰$ (Fig. 3g and h); and three closely associated individuals of cf. *Bigeminococcus mucidus* have $\delta^{13}C$ ranging from $-22.3‰$ to $-24.9‰$ (Fig. 3e and f). In comparison with the previous SIMS-study of Bitter Springs fossils by House et al. (2000), which for 15 fossils reported a range in $\delta^{13}C$ of $-21.0‰$ to $-31.9‰$ (average $= -26.4‰$; Fig. 1), the nine Bitter Springs specimens analyzed here are isotopically less variable and, on average, higher in $\delta^{13}C$.

3.2.3. Min'Yar Formation

In a ~1-mm^2-area of a vertically sectioned stromatolitic microbial mat from the ~740 Ma Min'Yar chert, 20 individual microfossils representing five cyanobacterial taxa, both coccoidal and filamentous, were analyzed (Fig. 4). The $\delta^{13}C$ values measured range from $-23.5‰$ to $-34.6‰$, analyzed within three brackets having an average external precision of $\pm 1.9‰$ (2 SD). The most prominent feature of the area studied is an extensive platy colony of the coccoidal cyanobacterium *Glenobotrydion majorinum*

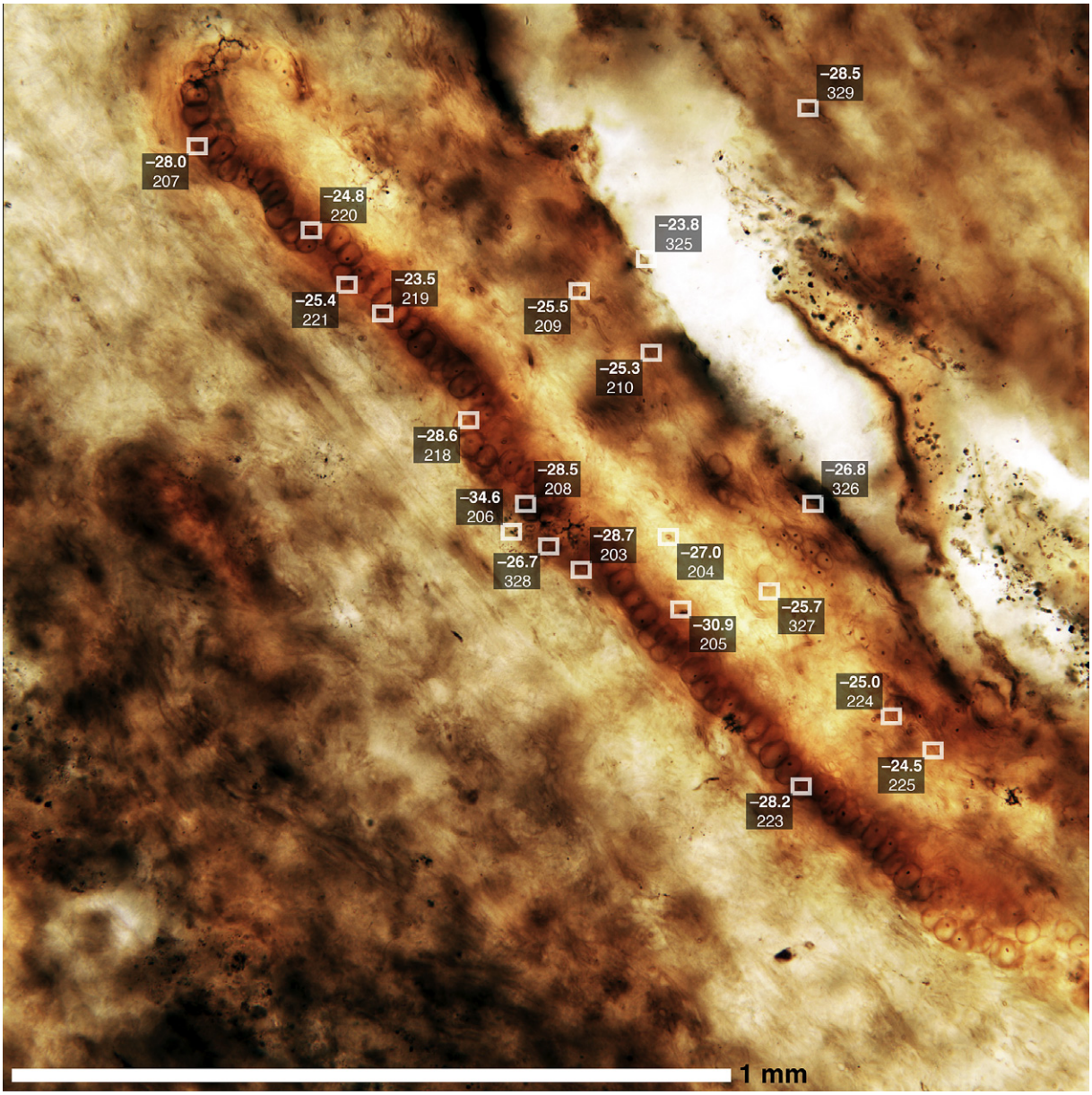

Fig. 4. Carbon isotope analyses of a fossil microbial mat from the Min'yar Formation. Targets analyzed are indicated by open rectangles; carbon isotope ratios (‰, VPDB) and individual analysis numbers are shown in gray boxes.

composed of hundreds of cells. In addition to exhibiting well preserved cell walls, the individual cells of the colony commonly contain a single, typically centrally located, ~1 μm-diameter spheroidal body of concentrated carbonaceous matter (Fig. 4), presumably condensed cytoplasmic remnants. Analyses of six *G. majorinum* cells that did not sample such intracellular bodies yielded a $\delta^{13}C$ value of $-25.5 \pm 2.4‰$. In contrast, measurements on cells that sampled such bodies yielded lower $\delta^{13}C$: for three such cells a $\delta^{13}C$ value of $-28.4 \pm 0.2‰$ (lower by ~3‰, outside 2 SD analytical precision), and for one other central body-containing cell, −34.6‰. A *t*-test on the two populations (cells with and cells without an internal body; unpaired, one tail, unequal variances) demonstrates that the different $\delta^{13}C$ values are statistically significant at the 95% confidence level ($p = 0.035$).

Four specimens of a second colonial coccoidal cyanobacterium, cf. *Gloeodiniopsis lamellosa*, easily distinguishable from *G. majorinum* by its occurrence in colonies of only a few cells that are enclosed by multilamellated envelopes, yielded a $\delta^{13}C$ value of $-29.1 \pm 1.8‰$. Five analyses of *Eomycetopsis robusta*, the originally carbohydrate-rich extracellular tubular sheaths of a filamentous oscillatoriacean cyanobacterium, yielded a $\delta^{13}C$ value of $-25.5 \pm 1.5‰$ (higher by 3.6‰, outside 2 SD precision). A *t*-test on the two populations (*G. lamellosa* and *E. robusta*; unpaired, one tail, unequal variances) demonstrates that the different $\delta^{13}C$ values are statistically significant ($p = 0.002$). Fig. 5 shows a frequency histogram that summarizes $\delta^{13}C$ measurements of the Min'yar fossils and their taxonomic and microstructural correlations (see Section 4).

3.2.4. Chichkan Formation

In a single bracket having an external precision of 1.6‰ (2 SD), five microfossils from two samples of the ~775 Ma Chichkan Formation were analyzed, specimens that included filamentous and coccoidal cyanobacteria as well as phytoplanktonic eukaryotic acritarchs. In one of these samples (dissected from thin section 4681-68B 7A-2), three individual microfossils were each analyzed in replicate. Two analyses of a single specimen of *Siphonophycus solidum*, the extracellular tubular sheath of an oscillatoriacean cyanobacterium, yielded an average $\delta^{13}C$ of −31.3‰ (Fig. 6). Five analyses were made of a single specimen of *Oscillatoriopsis media*, the cellular trichome of an oscillatoriacean like that producing the analyzed *S. solidium* sheath. Four of

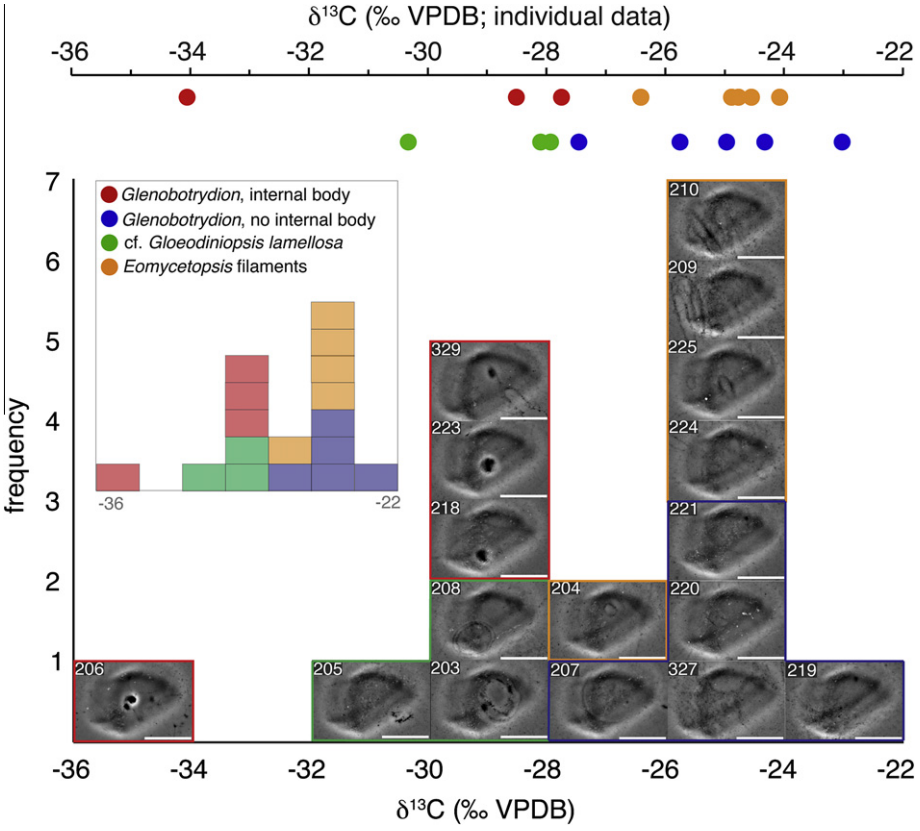

Fig. 5. Frequency histogram showing backscattered electron images of SIMS analytical pits and the distribution of carbon isotope ratios correlated with the taxonomy and anatomic microstructure of the Min'yar Formation microfossils. Individual analysis numbers are indicated at the top left of each image. Analyses 203, 205, and 208 (in the inset, highlighted in green) sampled the multilamellated-envelope enclosed spherical taxon cf. *Gloeodiniopsis lamellosa* and show lower $\delta^{13}C$ compared to the filamentous morphotype *Eomycetopsis robusta* (209, 210, 224–225; highlighted in orange). Analyses 206, 218, 223, and 329 (highlighted in red) sampled the internal body of *Glenobotrydion majorinum* cells and show lower $\delta^{13}C$ than analyses of *G. majorinum* cells that did not sample such bodies (207, 219–221, and 327; highlighted in blue). Individual data are shown at top of figure, color-coded as indicated above. See inset histogram for key to color coded categories.

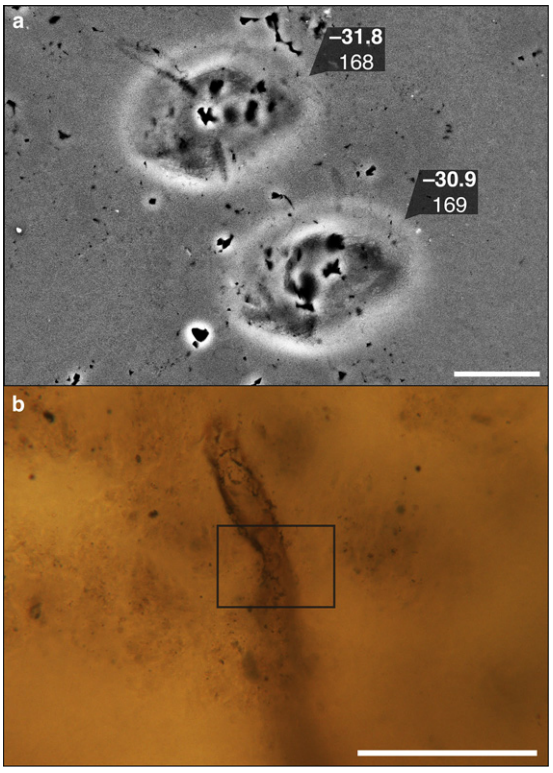

Fig. 6. Backscattered electron image (a) and transmitted light image (b) showing SIMS carbon isotope analyses of *Siphonopycus solidum* from the Chichkan Formation. Gray rectangle in (b) shows area enlarged in (a). Carbon isotope ratios (‰, VPDB) and individual analysis numbers are shown next to analytical pits in (a); scale bars represent 10 μm in (a) and 100 μm in (b).

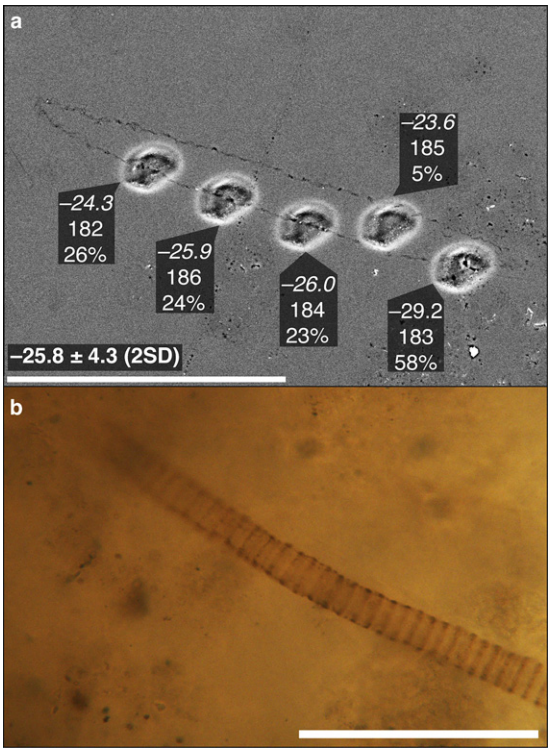

Fig. 7. Backscattered electron image (a) and transmitted light image (b) showing SIMS carbon isotope analyses of *Oscillatoriopsis media* from the Chichkan Formation. In (a), carbon isotope ratios (‰, VPDB), individual analysis numbers, and ^{12}C count rates relative to bracketing standard are shown next to analytical pits. Scale bars represent 100 μm. Analysis 183 sampled organic matter that appears distinct from, and has lower $\delta^{13}C$ than the cell walls sampled in the other four analyses (182, 184–186), which have $\delta^{13}C$ values consistent with cyanobacterial photosynthesis.

these, which sampled only the trichomic cell walls and have ^{12}C count rates $< 27\%$ of bracketing standards, yielded an average $\delta^{13}C$ of $-24.9‰$, whereas the fifth analysis, having a high relative ^{12}C count rate (58%) and yielding a $\delta^{13}C$ value of $-29.2‰$, appears to have also sampled an associated organic phase with lower $\delta^{13}C$ (presumably, the flocculent particulate kerogen in which the specimen is embedded; Fig. 7). Notably, bulk $\delta^{13}C$ of the Chichkan Fm is similar to this phase, at $-28.4 \pm 0.5‰$. Two analyses of a third specimen from this sample, the relatively large-celled phytoplanktonic acritarch *Leiosphaerida crassa*, have an average $\delta^{13}C$ value of $-30.8‰$ (Fig. 8).

In the other sample of the stromatolitic Chichkan chert (dissected from thin section 4681-68B 7A-1), specimens of both a large-celled acritarch (*L. crassa*) and a four-celled cyanobacterial colony (*Myxococcoides* sp.) situated ~8 mm apart, were analyzed three times each. As shown in Fig. 9, measurements of the acritarch yielded a $\delta^{13}C$ value of $-28.9 \pm 1.0‰$ whereas those of the colonial cyanobacterium yielded a $\delta^{13}C$ of $-22.6 \pm 0.5‰$.

4. DISCUSSION

Among the major factors that can influence the carbon isotopic composition of fossilized autotrophic microorganisms are (1) syn- or post-depositional diagenetic effects, (2) the isotopic fractionation associated with autotrophic carbon fixation ($\varepsilon_P = \delta^{13}C_{substrate} - \delta^{13}C_{fixed\ carbon}$), (3) the isotopic composition of the original carbon substrate (e.g., dissolved inorganic carbon), and (4) the isotopic fractionation associated with post-fixation (anabolic) biosynthetic processes ($\varepsilon_B = \delta^{13}C_{fixed\ \ carbon} - \delta^{13}C_{anabolite}$). Each of these factors is addressed in turn below.

4.1. Diagenesis and Preservation

We first consider the preservational and diagenetic context of the microfossils investigated in this study. All of the specimens analyzed were included in an earlier systematic study of 25 geological units demonstrating that Raman spectroscopy can provide, at sub-micrometer spatial resolution, in situ non-destructive chemical-structural characterization of the carbonaceous components of chert-permineralized individual Precambrian microfossils. In addition, this study introduced the Raman Index of Preservation (RIP), a quantitative measure of the geochemical maturity of such components (Schopf et al., 2005). The four fossiliferous cherts chosen for the present study are those having the highest RIP values (8.6–9.0) from the Schopf et al. (2005) study, indicating that the kerogen that

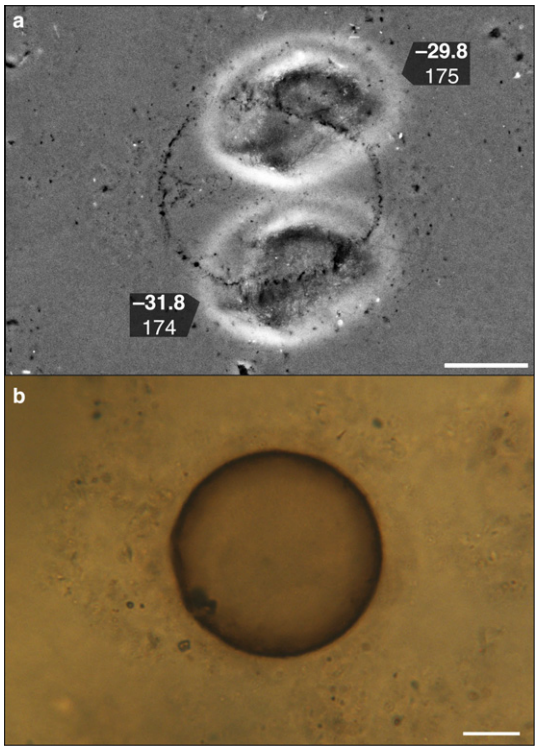

Fig. 8. Backscattered electron image (a) and transmitted light image (b) showing SIMS carbon isotope analyses of *Leiosphaerida crassa* from the Chichkan Formation. In (a), carbon isotope ratios (‰, VPDB) and individual analysis numbers are shown next to analytical pits; scale bars represent 10 μm.

comprises the fossils here analyzed is among the best preserved (least geochemically altered) documented from the Precambrian record. The carbonaceous components of the Chichkan chert fossils have also been characterized by a variety of methods including atomic force microscopy (Kempe et al., 2002), focused ion beam sectioning (Kempe et al., 2005), confocal laser scanning microscopy (Schopf et al., 2010b), and transmission electron microscopy (Moczydlowska et al., 2010); the elemental compositions of Bitter Springs fossils have been measured using NanoSIMS ion imaging (Oehler et al., 2009).

Early diagenetic decomposition could also have affected the isotopic composition of microfossils. Heterotrophic processing of primary production biomass (preserved as cyanobacteria or eukaryotic phytoplankton) could lead to a slight increase in $\delta^{13}C$ of microfossils due to the preferential assimilation of labile components (lipids and proteins) with lower $\delta^{13}C$. The familiar phrase "you are what you eat (plus a few ‰)" (Deniro and Epstein, 1978) describing the typical relation of heterotrophic biomass to food source implies that the change in $\delta^{13}C$ of the food source during heterotrophic alteration is small. Indeed, the increase in $\delta^{13}C$ of organic matter preserved in marine sediments due to bacterial heterotrophy is thought to range from 1‰ to 2‰, but can be as high as 3–5‰ at the level of individual compounds (when cellular structures are no longer evident, and particularly in Phanerozoic and modern environments where processing by zooplankton is a significant factor) (Hayes, 1993). In cyanobacteria, selective preservation of sheath biomass relative to cell biomass during heterotrophic microbial decomposition (Bartley, 1996) could further

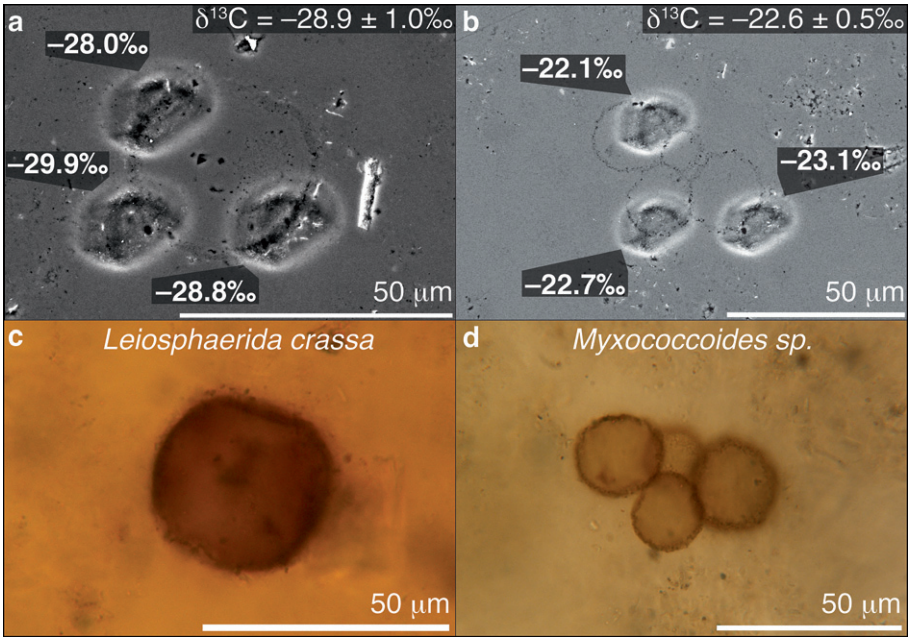

Fig. 9. Backscattered electron (a, b) and transmitted light (c, d) images showing SIMS carbon isotope analyses of *Leiosphaerida crassa* (a, c) and *Myxococcoides* sp. (b, d), microfossils situated ~8 mm apart in the same thin section of the Chichkan Formation stromatolitic chert. In (a) and (b), carbon isotope ratios ($\delta^{13}C$, ‰ VPDB) are shown next to analytical pits, and the average and total range of $\delta^{13}C$ values are indicated at top right. Scale bars represent 50 μm. The specimen of *L. crassa* has $\delta^{13}C$ consistent with eukaryotic photosynthesis, whereas that of *Myxococcoides* sp. is consistent with cyanobacterial photosynthesis.

contribute to a net increase in $\delta^{13}C$ of total microfossil biomass due to the biosynthetic processes discussed below. The excellent preservation of the specimens reported here (in fact, the presence of cellular structure in general) argues that any effect of heterotrophic alteration on $\delta^{13}C$ was small (<3‰).

4.2. Carbon fixation

A second factor affecting the carbon isotopic composition of fossil microbial autotrophs is the fractionation associated with carbon fixation ($\varepsilon_P = \delta^{13}C_{substrate} - \delta^{13}C_{fixed\ carbon}$). In this regard, the range of $\delta^{13}C$ observed among microfossils analyzed in the present study (−34.6‰ to −22.1‰) is uniformly consistent with carbon fixation via the Calvin cycle, that is, fixation by ribulose bisphosphate carboxylase (RuBisCO) (Preuß et al., 1989; House et al., 2000). As House et al. (2000) noted, microfossil $\delta^{13}C$ values ranging from −20‰ to −35‰ in the absence of morphological evidence do not demonstrate definitively that the organisms in question fixed carbon via the Calvin cycle, as other metabolisms (e.g., the acetyl-CoA pathway) can produce similar isotopic fractionations (Fuchs et al., 1979; Schidlowski et al., 1983; Preuß et al., 1989). However, the $\delta^{13}C$ values in combination with previous morphology-based taxonomy (Barghoorn and Tyler, 1965; Schopf, 1968; Schopf and Blacic, 1971; Sergeev and Schopf, 2010), support the conclusion that the fossil organisms here analyzed fixed carbon by RuBisCO.

Laboratory experiments with living phytoplankton show that ε_P associated with carbon fixation by RuBisCO decreases from maximum values for the enzymatic system as a result of environmental and physiological factors that limit the ability of a cell to concentrate the carbon substrate. Substrate availability is directly proportional to the concentration of dissolved CO_2 (CO_2(aq)) and inversely proportional to growth rate (μ), leading to the relation ε_P μ/CO_2(aq) (Laws et al., 1997). Cell geometry also plays a crucial role in determining ε_P: flux of CO_2(aq) into a cell is strongly related to the surface to volume ratio which decreases with increasing growth rate to a characteristic maximum value for a taxon (Popp et al., 1998). Other environmental factors, including nutrient availability, can have important effects (Cassar et al., 2006). Some of the variability in microfossil $\delta^{13}C$ observed within individual geologic units may be explained by these environmental and physiological controls on ε_P.

4.3. Substrate

A third factor affecting the $\delta^{13}C$ of preserved microfossils is the isotopic composition of their carbon substrate (e.g., CO_2(aq) or HCO_3^-), a value that can be estimated by measuring the $\delta^{13}C$ of sedimentary carbonates and assuming equilibrium fractionation at a given temperature (Emrich and Vogel, 1970). Although modern cyanobacteria have carbon concentration mechanisms that allow them to uptake either CO_2 or HCO_3^- (Badger and Price, 2003), we focus here on fixation via CO_2 for the sake of simplicity. For the present study, we have used whole rock (bulk) $\delta^{13}C$ measurements of stromatolitic chert-associated carbonates from the Gunflint (−2.9‰) and Bitter Springs (3.4‰) Formations reported by Strauss and Moore (1992), and the average value (1.3‰) of 15 such measurements reported by Podkovyrov et al. (1998) from the Upper Subformation of the Min'Yar Formation. For the Chichkan Formation, we report that small (~10–30 μm) calcite crystals in the fossil-bearing cherts here studied have a $\delta^{13}C = -12.8 \pm 0.2$‰ (VPDB) and $\delta^{18}O = -11.5 \pm 0.1$‰ (VPDB) (analyzed by phosphoric acid digestion at the University of Washington IsoLab, Department of Earth and Space Sciences; pers. comm. A. Schauer), unusually low $\delta^{13}C$ and $\delta^{18}O$ values for carbonates of Chichkan age (e.g., Strauss et al., 1992) that we interpret to evidence either diagenetic alteration by a low $\delta^{13}C$ and $\delta^{18}O$ fluid or the incorporation of isotopically light, remineralized carbon in sediments during deposition. It is thus unlikely that these Chichkan carbonates faithfully record the $\delta^{13}C$ of photic zone DIC, and these data have therefore been excluded from our analyses.

Fig. 10 shows a strong correlation between bulk $\delta^{13}C$ of carbonate ($\delta^{13}C_{carb}$) and average in situ $\delta^{13}C$ of microfossils analyzed from the Gunflint, Min'yar, and Bitter Springs Formations. If equilibrium fractionation between CO_2(aq) in the photic zone and solid carbonate deposited in coeval sediments is assumed for each of these units, these $\delta^{13}C_{carb}$ data can be used to estimate the $\delta^{13}C$ of CO_2(aq) in the photic zone for a given temperature (with a dependence of −0.063‰/°C) (Emrich and Vogel, 1970). These values can then be used to calculate ε_P for each of the microfossil measurements reported here. Given these assumptions, average ε_P (at 20 °C) is calculated for the Gunflint, Bitter

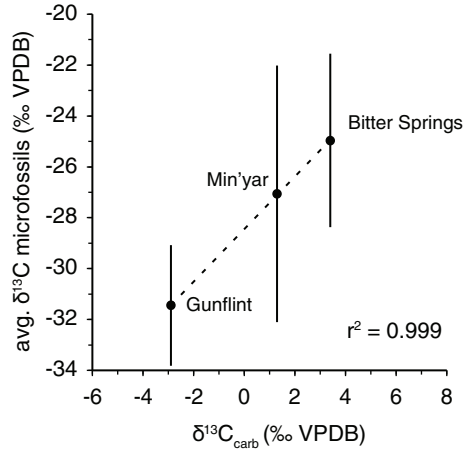

Fig. 10. Average $\delta^{13}C$ of in situ carbon isotope analyses of cyanobacterial microfossils versus $\delta^{13}C$ of carbonates from three of the Proterozoic formations studied. The total range of microfossil $\delta^{13}C$ measured is indicated by vertical bars for each formation, and a least squares regression fit to the average values is shown by the dotted line. For all three units, fractionation between carbonate and kerogen in individual microfossils ($\Delta^{13}C_{carb-org}$) is remarkably constant (28.4 ± 2‰, 1 SD). Assuming equilibrium isotope fractionation between dissolved CO_2 in the photic zone and solid carbonate, the average photosynthetic fractionation effect ($\varepsilon_P = \Delta^{13}C_{DIC-org}$) for microfossils classified as cyanobacteria in these units is ~19‰.

Springs, and Min'yar Formations to be 18.6‰, 18.3‰, and 18.3‰, respectively. For temperatures between 15 and 30 °C, calculated ε_P values for individual microfossils in these three units range from 14.4‰ to 26.6‰.

4.4. Biosynthesis

A fourth factor affecting the $\delta^{13}C$ of preserved organic-walled microorganisms is the nature of their biosynthetic processes. Laboratory experiments show that for cyanobacteria the ε_P for carboxylation of ribulose bisphosphate is typically 16–22‰ (Guy et al., 1993; Sakata et al., 1997; Popp et al., 1998) but for eukaryotes ranges up to 29‰ (Roeske and Oleary, 1985). Thus, the estimated ε_P of 18–19‰ for microfossils from the Gunflint, Bitter Springs, and Min'yar formations is consistent with the morphology-based cyanobacterial affinity inferred for the taxa analyzed (Barghoorn and Tyler, 1965; Schopf, 1968; Schopf and Blacic, 1971). Similarly, three analyses of a four-celled cyanobacterial colony (*Myxococcoides* sp.) from the Chichkan Formation yielded $\delta^{13}C$ values consistent with cyanobacterial photosynthesis (-22.6 ± 1.0‰; Fig. 9). In contrast with this cyanobacterium, however, replicate analyses of two Chichkan specimens of the relatively large unicellular acritarch *L. crassa* (one of them situated ~8 mm distant from the cyanobacterial colony in the same thin section) yielded $\delta^{13}C$ values of -30.8 ± 1.0‰ and -28.9 ± 1.0‰ that document a relatively ^{13}C-depleted composition consistent with the morphological classification of these organisms as eukaryotic algal phytoplankton (Figs. 8 and 9).

Establishing whether morphologically simple leiosphaerid microfossils are eukaryotes or large cyanobacterial sheaths has to date required analysis of the micro- and nanoscale ultrastructure of their cell walls with techniques such as transmission electron microscopy (Javaux et al., 2004; Moczydlowska et al., 2010) and atomic force microscopy (Kempe et al., 2002; Kempe et al., 2005). In situ carbon isotope measurements of specimens in the Chichkan Formation offer a valuable complement to such morphological analysis in establishing biological affinity, and these data suggest that biosynthetic differences observed between living microorganisms of the bacterial and eukaryotic domains were similar in the Precambrian and are preserved isotopically in ancient organic-walled microfossils.

Specimens analyzed in the stromatolitic microbial mat of the Min'yar chert exhibit variability in carbon isotopic composition that correlates both with microfossil taxonomy and microbial anatomic microstructure (Figs. 6 and 7). Four individuals of the multilamellated envelope-enclosed taxon (cf. *G. lamellosa*) have $\delta^{13}C$ values between −30.9‰ and −28.3‰. Five analyses of the filamentous tubular morphotype *E. robusta* yielded $\delta^{13}C$ values ranging from −27.0‰ to −24.5‰ (avg. −25.5‰). Analyses of the spheroidal species *G. majorinum* that sampled only cell walls (and not their distinctive intracellular bodies) have an average $\delta^{13}C$ value of −25.9‰, similar to that of *E. robusta* (for which, similarly, only exterior walls were sampled), a value ~2.5‰ higher than the average of four analyses of *G. majorinum* cells that sampled the internal body (avg. −28.4‰).

Is the measured ^{12}C-enrichment of the intracellular bodies relative to cell walls of these *G. majorinum* cells an analytical artifact or the preserved signal of an original biosynthetic fractionation effect? Kerogen in the intracellular bodies and cell walls is amorphous, so an orientation effect (such as that observed for $\delta^{13}C$ analysis of graphite) can be ruled out. As discussed previously, a correlation between H/C and instrumental bias has been observed in SIMS $\delta^{13}C$ analysis of kerogen using a less intense (0.5 nA) beam than that applied in this study (2.5 nA) (Sangély et al., 2005; Williford et al., 2011). We observe no such relation in our measurements of carbonaceous cherts with varying H/C using the 2.5 nA beam (Fig. S12). However, average $^{13}CH/^{13}C$ for analyses that sampled an internal body (0.76) is different than that for analyses that sampled only cell walls (0.05), and there is a negative correlation between $^{13}CH/^{13}C$ and $\delta^{13}C$ ($r^2 = 0.63$) for all analyses of *G. majorinum*. The correlation is dominated by a single point with low $\delta^{13}C$, without which r^2 decreases to 0.33. Such a correlation could be produced in the absence of an H/C effect on bias if the OM in the internal bodies was simply more lipid (and thus H) rich than OM in the cell walls of *G. majorinum*, and the original biosynthetic fractionation was preserved, consistent with our interpretations (below). However, if we assume that the variability in both H/C and $\delta^{13}C$ is random in the two populations, we can apply a correction based upon a correlation between bias and H/C that we observe for kerogen analyses using a 0.5 nA beam. It must be stressed that this is only a sensitivity analysis and we do not use, nor do we advocate, such bias corrections across such widely varying analytical conditions and different analytical sessions for other purposes. When such a correction is applied in this case, the average $\delta^{13}C$ value of analyses sampling internal bodies increases by 0.9‰, and that of analyses sampling only cell walls increases by 0.1‰. When the *t*-test described above (see Section 3) is performed for the "corrected" values, the new *p*-value is 0.055. The sample sizes are small, necessitating "statistics of small numbers," but on the basis of the preceding exercise and the "uncorrected" *t*-test, we conclude that the difference in $\delta^{13}C$ between analyses of *G. majorinum* sampling internal bodies and those sampling only cell walls is highly unlikely to be due to analytical artifacts.

Among modern microorganisms, including both cyanobacteria (Sakata et al., 1997; Jahnke et al., 2004; Wieland et al., 2008) and eukaryotic phytoplankton (Schouten et al., 1998; Riebesell et al., 2000), lipids are depleted in ^{13}C by several permil relative to total biomass. In contrast, $\delta^{13}C$ of carbohydrates (including extracellular polymeric substances such as those of cyanobacterial sheaths), amino acids, and cyanobacterial exudates is commonly higher than total biomass (Wieland et al., 2008). Given these data, it seems likely that the relatively ^{13}C-depleted intracellular bodies of *G. majorinum* originally incorporated appreciable amounts of membrane lipids and that the kerogen of which they are composed has preserved a biosynthetically produced isotopic signature with lower $\delta^{13}C$ than that of their originally peptidoglycan cell walls.

Similarly, if our interpretation of the ε_P values of the Chichkan cyanobacterial colony and the eukaryotic acrit-

archs is correct, the results of two analyses of *S. solidum* (avg. $\delta^{13}C = -31.3$; Fig. 6) and one of the five analyses of *O. media* with a $\delta^{13}C$ of $-29.2‰$ (Fig. 7) from this unit may also record evidence of biosynthetic effects. Both of these taxa are classified as cyanobacteria – *S. solidum* as the tubular extracellular sheath of an oscillatoiacean trichome such as *O. media* – and if ε_P was the dominant factor that determined $\delta^{13}C$, both of these microfossils should have higher $\delta^{13}C$ than the Chichkan specimens of the protistan eukaryotic acritarch *L. crassa* (as is the case with the colonial *Myxococcoides* sp.; Fig. 9). For *O. media*, the four analyses that sampled only its cell walls (at relatively low ^{12}C count rates) have $\delta^{13}C$ values consistent with a cyanobacterial peptidoglycan composition. The single other analysis of this fossil appears to have sampled an additional organic phase, separate from the cell wall and most likely the flocculent particulate kerogen in which the specimen is embedded (Fig. 7), that has an isotopically light carbon signature. As discussed above, if this phase were originally lipid-rich, its sampling would explain the relatively low $\delta^{13}C$ value. Analyses of the specimen of *S. solidum*, inferred to be a cyanobacterial sheath (and dominantly composed of carbohydrates), also appear to have sampled this low $\delta^{13}C$ background organic phase (Fig. 6). Interpretation of *S. solidum* as a cyanobacterial sheath implies that the microfossil in question should be isotopically similar to cyanobacterial cell wall material or extracellular polymeric substances, similar to the bulk biomass of such cyanobacteria, and ^{13}C-enriched relative to their lipids.

5. CONCLUSIONS

In situ carbon isotope analyses of 46 well-preserved microfossils from the Proterozoic Gunflint, Bitter Springs, Min'yar, and Chichkan Formations yielded $\delta^{13}C$ values ranging from $-34.6‰$ to $-22.1‰$, consistent with RuBisCO-mediated photosynthetic carbon fixation. The average $\delta^{13}C$ values of microfossils classified on the basis of their morphology as cyanobacteria, considered together with those of carbonates from the same units, documents an isotopic offset consistent with the known fractionation effect of cyanobacterial oxygenic photoautotrophy ($\varepsilon_P \approx 20‰$). Carbon isotope variability of the fossils analyzed in this study correlates with their morphology-based taxonomy and may preserve evidence of fractionation effects related to lipid and peptidoglycan biosynthesis linked to internal microstructures within single fossil cells. Replicate measurements of a colonial cyanobacterium and a leiosphaerid acritarch in close spatial association within a single sample of the Chichkan Formation (~775 Ma) suggest that SIMS-based isotopic analysis discriminates between the preserved products of cyanobacterial and eukaryotic RuBisCO-driven photosynthesis and thus contributes to the resolution of morphological ambiguity in permineralized organic-walled microfossils of Proterozoic age.

ACKNOWLEDGMENTS

We thank Noriko Kita, Jim Kern, and Reinhard Kozdon for assistance with the ion microprobe, John Fournelle for assistance with the SEM, Andy Czaja and Clark Johnson for helpful discussions, and Brian Hess for expert sample preparation. The loan of carbonaceous chert sample PPRG 215-1 by Christopher H. House (Penn State University) was critical to the completion of this study. We thank Andrew Schauer and IsoLab in the Department of Earth and Space Sciences at the University of Washington for providing the carbon and oxygen isotope analyses of the Chichkan Formation carbonates. Constructive comments from Profs. Trevor Ireland (A.E.), Malcom Walter, David Fike, and one anonymous reviewer improved the manuscript. Funding for this study was provided by the NASA Astrobiology Institute. The WiscSIMS Lab is partially funded by NSF-EAR (0319230, 0744079, 1053466).

APPENDIX A. SUPPLEMENTARY DATA

Supplementary data associated with this article can be found, in the online version, at http://dx.doi.org/10.1016/j.gca.2012.11.005.

REFERENCES

Badger M. R. and Price G. D. (2003) CO_2 concentrating mechanisms in cyanobacteria: molecular components, their diversity and evolution. *J. Exp. Bot.* **54**, 609–622.

Barghoorn E. S. and Tyler S. A. (1965) Microorganisms from Gunflint Chert. *Science* **147**, 563–577.

Bartley J. K. (1996) Actualistic taphonomy of cyanobacteria: implications for the Precambrian fossil record. *Palaios* **11**, 571–586.

Cassar N., Laws E. A. and Popp B. N. (2006) Carbon isotopic fractionation by the marine diatom *Phaeodactylum tricornutum* under nutrient- and light-limited growth conditions. *Geochim. Cosmochim. Acta* **70**, 5323–5335.

Deniro M. J. and Epstein S. (1978) Influence of diet on the distribution of carbon isotopes in animals. *Geochim. Cosmochim. Acta* **42**, 495–506.

Eiler J. M., Graham C. and Valley J. W. (1997) SIMS analysis of oxygen isotopes: matrix effects in complex minerals and glasses. *Chem. Geol.* **138**, 221–244.

Emrich K. and Vogel J. C. (1970) Carbon isotope fractionation during precipitation of calcium carbonate. *Earth Planet. Sci. Lett.* **8**, 363–371.

Fralick P., Davis D. W. and Kissin S. A. (2002) The age of the Gunflint Formation, Ontario, Canada: single zircon U–Pb age determinations from reworked volcanic ash. *Can. J. Earth Sci.* **39**, 1085–1091.

Fuchs G., Thauer R., Ziegler H. and Stichler W. (1979) Carbon isotope fractionation by *Methanobacterium thermoautotrophicum*. *Arch. Microbiol.* **120**, 135–139.

Guy R. D., Fogel M. L. and Berry J. A. (1993) Photosynthetic fractionation of the stable isotopes of oxygen and carbon. *Plant Physiol.* **101**, 37–47.

Hayes J. M. (1993) Factors controlling C-13 contents of sedimentary organic-compounds – principles and evidence. *Mar. Geol.* **113**, 111–125.

Hayes J. M., Kaplan I. R. and Wedeking K. W. (1983) Precambrian organic geochemistry, preservation of the record. In *The Earth's Earliest Biosphere: Its Origin and Evolution* (ed. J. W. Schopf). Princeton University Press, Princeton, New Jersey, pp. 93–134.

Hindie E., Coulomb B. and Galle P. (1992) SIMS microscopy – a tool to measure the intracellular concentration of carbon-14-labeled molecules. *Biol. Cell* **74**, 89–92.

House C. H., Schopf J. W., McKeegan K. D., Coath C. D., Harrison T. M. and Stetter K. O. (2000) Carbon isotopic composition of individual Precambrian microfossils. *Geology* **28**, 707–710.

Huberty J. M., Kita N. T., Kozdon R., Heck P. R., Fournelle J. H., Spicuzza M. J., Xu H. F. and Valley J. W. (2010) Crystal orientation effects in delta O-18 for magnetite and hematite by SIMS. *Chem. Geol.* **276**, 269–283.

Jahnke L. L., Embaye T., Hope J., Turk K. A., Van Zuilen M., Des Marais D. J., Farmer J. D. and Summons R. E. (2004) Lipid biomarker and carbon isotopic signatures for stromatolite-forming, microbial mat communities and Phormidium cultures from Yellowstone National Park. *Geobiology* **2**, 31–47.

Javaux E. J., Knoll A. H. and Walter M. R. (2004) TEM evidence for eukaryotic diversity in mid-Proterozoic oceans. *Geobiology* **2**, 121–132.

Kaufman A. J. and Xiao S. H. (2003) High CO_2 levels in the Proterozoic atmosphere estimated from analyses of individual microfossils. *Nature* **425**, 279–282.

Kempe A., Schopf J. W., Altermann W., Kudryavtsev A. B. and Heckl W. M. (2002) Atomic force microscopy of Precambrian microscopic fossils. *Proc. Natl. Acad. Sci. USA* **99**, 9117–9120.

Kempe A., Wirth R., Altermann W., Stark R. W., Schopf J. W. and Heckl W. A. (2005) Focussed ion beam preparation and in situ nanoscopic study of Precambrian acritarchs. *Precambr. Res.* **140**, 36–54.

Kennedy C. B., Gault A. G., Fortin D., Clark I. D., Pedersen K., Scott S. D. and Ferris F. G. (2010) Carbon isotope fractionation by circumneutral iron-oxidizing bacteria. *Geology* **38**, 1087–1090.

Kita N. T., Ushikubo T., Fu B. and Valley J. W. (2009) High precision SIMS oxygen isotope analysis and the effect of sample topography. *Chem. Geol.* **264**, 43–57.

Kozdon R., Kita N. T., Huberty J. M., Fournelle J. H., Johnson C. A. and Valley J. W. (2010) In situ sulfur isotope analysis of sulfide minerals by SIMS: precision and accuracy, with application to thermometry of similar to 3.5 Ga Pilbara cherts. *Chem. Geol.* **275**, 243–253.

Laws E. A., Bidigare R. R. and Popp B. N. (1997) Effect of growth rate and CO_2 concentration on carbon isotopic fractionation by the marine diatom *Phaeodactylum tricornutum*. *Limnol. Oceanogr.* **42**, 1552–1560.

McKeegan K. D., Walker R. M. and Zinner E. (1985) Ion microprobe isotopic measurements of individual interplanetary dust particles. *Geochim. Cosmochim. Acta* **49**, 1971–1987.

Moczydlowska M., Schopf J. W. and Willman S. (2010) Micro- and nano-scale ultrastructure of cell walls in Cryogenian microfossils: revealing their biological affinity. *Lethaia* **43**, 129–136.

Oehler D. Z., Robert F., Walter M. R., Sugitani K., Allwood A., Meibom A., Mostefaoui S., Selo M., Thomen A. and Gibson E. K. (2009) NanoSIMS: insights to biogenicity and syngeneity of Archaean carbonaceous structures. *Precambr. Res.* **173**, 70–78.

Pace N. R. (1997) A molecular view of microbial diversity and the biosphere. *Science* **276**, 734–740.

Planavsky N., Rouxel O., Bekker A., Shapiro R., Fralick P. and Knudsen A. (2009) Iron-oxidizing microbial ecosystems thrived in late Paleoproterozoic redox-stratified oceans. *Earth Planet. Sci. Lett.* **286**, 230–242.

Podkovyrov V. N., Semikhatov M. A., Kuznetsov A. B., Vinogradov D. P., Kozlov V. I. and Kislova I. V. (1998) Carbonate carbon isotopic composition in the upper Riphean stratotype, the Karatau group, southern Urals. *Stratigr. Geol. Correl.* **6**, 319–335.

Popp B. N., Laws E. A., Bidigare R. R., Dore J. E., Hanson K. L. and Wakeham S. G. (1998) Effect of phytoplankton cell geometry on carbon isotopic fractionation. *Geochim. Cosmochim. Acta* **62**, 69–77.

Preuß A., Schauder R., Fuchs G. and Stichler W. (1989) Carbon isotope fractionation by autotrophic bacteria with 3 different CO_2 fixation pathways. *Z. Naturforsch. C: J. Biosci.* **44**, 397–402.

Riebesell U., Revill A. T., Holdsworth D. G. and Volkman J. K. (2000) The effects of varying CO_2 concentration on lipid composition and carbon isotope fractionation in *Emiliania huxleyi*. *Geochim. Cosmochim. Acta* **64**, 4179–4192.

Roeske C. A. and Oleary M. H. (1985) Carbon isotope effect on carboxylation of ribulose bisphosphate catalyzed by ribuolose bisphosphate carboxylase from *Rhodospirillum rubrum*. *Biochemistry* **24**, 1603–1607.

Rothschild L. J. and Mancinelli R. L. (2001) Life in extreme environments. *Nature* **409**, 1092–1101.

Sakata S., Hayes J. M., McTaggart A. R., Evans R. A., Leckrone K. J. and Togasaki R. K. (1997) Carbon isotopic fractionation associated with lipid biosynthesis by a cyanobacterium: relevance for interpretation of biomarker records. *Geochim. Cosmochim. Acta* **61**, 5379–5389.

Sangély L., Chaussidon M., Michels R. and Huault V. (2005) Microanalysis of carbon isotope composition in organic matter by secondary ion mass spectrometry. *Chem. Geol.* **223**, 179–195.

Schidlowski M., Hayes J. and Kaplan I. (1983) Isotopic inferences of ancient biochemistries: carbon, sulfur, hydrogen, and nitrogen. In *The Earth's Earliest Biosphere* (ed. J. Schopf). Princeton University Press, Princeton, New Jersey, pp. 149–185.

Schopf J. W. (1968) Microflora of the Bitter Springs Formation. *J. Paleontol.* **42**, 651–688.

Schopf J. W. and Blacic J. M. (1971) New microorganisms from the Bitter Springs Formation (late Precambrian) of the north-central Amadeus Basin, Australia. *J. Paleontol.* **45**, 925–961.

Schopf J. W., Kudryavtsev A. B., Agresti D. G., Czaja A. D. and Wdowiak T. J. (2005) Raman imagery: a new approach to assess the geochemical maturity and biogenicity of permineralized Precambrian fossils. *Astrobiology* **5**, 333–371.

Schopf J. W., Kudryavtsev A. B., Sugitani K. and Walter M. R. (2010a) Precambrian microbe-like pseudofossils: a promising solution to the problem. *Precambr. Res.* **179**, 191–205.

Schopf J. W., Kudryavtsev A. B. and Sergeev V. N. (2010b) Confocal laser scanning microscopy and Raman imagery of the Late Neoproterozoic Chichkan microbiota of south Kazakhstan. *J. Paleontol.* **84**, 402–416.

Schouten S., Breteler W. C. M. K., Blokker P., Schogt N., Rijpstra W. I. C., Grice K., Baas M. and Damste J. S. S. (1998) Biosynthetic effects on the stable carbon isotopic compositions of algal lipids: implications for deciphering the carbon isotopic biomarker record. *Geochim. Cosmochim. Acta* **62**, 1397–1406.

Sergeev V. N. and Schopf J. W. (2010) Taxonomy, paleoecology and biostratigraphy of the Late Neoproterozoic Chichkan microbiota of south Kazakhstan: the marine biosphere on the eve of metazoan radiation. *J. Paleontol.* **84**, 363–401.

Strauss H. and Moore T. B. (1992) Abundances and isotopic compositions of carbon and sulfur species in whole rock and kerogen samples. In *The Proterozoic Biosphere: A Multidisciplinary Study* (eds. J. W. Schopf and C. Klein). Cambridge University Press, Cambridge, pp. 709–798.

Strauss H., Des Marais D. J., Hayes J. M. and Summons R. E. (1992) The carbon-isotopic record. In *The Proterozoic Biosphere: A Multidisciplinary Study* (eds. J. W. Schopf and C. Klein). Cambridge University Press, Cambridge, pp. 117–127.

Ueno Y., Isozaki Y., Yurimoto H. and Maruyama S. (2001) Carbon isotopic signatures of individual archean microfossils(?) from Western Australia. *Int. Geol. Rev.* **43**, 196–212.

Wacey D., Kilburn M. R., Saunders M., Cliff J. and Brasier M. D. (2011) Microfossils of sulphur-metabolizing cells in 3.4-billion-year-old rocks of Western Australia. *Nat. Geosci.* **4**, 698–702.

Walter M. R., Hofmann H. J. and Schopf J. W. (1983) Geographic and geologic data for processed rock samples. In *Earth's*

(ed. J. W. Schopf). Princeton University Press, Princeton, NJ, pp. 385–413.

Walter M. R., Veevers J. J., Calver C. R., Gorjan P. and Hill A. C. (2000) Dating the 840–544 Ma Neoproterozoic interval by isotopes of strontium, carbon, and sulfur in seawater, and some interpretative models. *Precambr. Res.* **100**, 371–433.

Ward P. and Brownlee D. (2000) *Rare Earth: Why Complex Life is Uncommon in the Universe*. Springer-Verlag, New York.

Wieland A., Pape T., Mobius J., Klock J. H. and Michaelis W. (2008) Carbon pools and isotopic trends in a hypersaline cyanobacterial mat. *Geobiology* **6**, 171–186.

Williford K. H., Ushikubo T., Lepot K., Hallmann C., Spicuzza M. J., Eigenbrode J. L., Summons R. E., Valley J. W. (2011) In situ carbon isotope analysis of Archean organic matter with SIMS, AGU Fall Meeting abs. B21E–0323.

Wilson J. P., Fischer W. W., Johnston D. T., Knoll A. H., Grotzinger J. P., Walter M. R., McNaughton N. J., Simon M., Abelson J., Schrag D. P., Summons R., Allwood A., Andres M., Gammon C., Garvin J., Rashby S., Schweizer M. and Watters W. A. (2010) Geobiology of the late Paleoproterozoic Duck Creek Formation, Western Australia. *Precambr. Res.* **179**, 135–149.

Associate editor: Trevor Ireland